arXiv:cond-mat/0506331v3 [cond-mat.other] 14 Jan 2006

Breathing mode of rapidly rotating Bose-Einstein condensates

Gentaro Watanabe[a,b]
[a] *NORDITA, Blegdamsvej 17, DK-2100 Copenhagen Ø, Denmark*
[b] *The Institute of Chemical and Physical Research (RIKEN),*
2-1 Hirosawa, Wako, Saitama 351-0198, Japan

(Dated: February 2, 2008)

We show that the breathing mode of a rapidly-rotating, harmonically-trapped Bose-Einstein condensate may be described by a generalized lowest Landau level (LLL) wave function, in which the oscillator length is treated as a variable. Using this wave function in a variational Lagrangian formalism, we show that the frequency of the breathing mode for a two-dimensional cloud is $2\omega_\perp$, where $\omega_\perp$ is the trap frequency. We also study large-amplitude oscillations and confirm that the above result is not limited to linear oscillations. The resulting mode frequency can be understood in terms of orbits of a single particle in a harmonic trap. The mode frequency is also calculated for a cloud in three dimensions and the result for the axial breathing mode frequency agrees with recent experimental data in the rapid rotation regime.

PACS numbers: 03.75.Kk, 05.30.Jp, 67.40.Vs, 47.37.+q

I. INTRODUCTION

The creation of vortices and vortex lattices in Bose-Einstein condensates of cold atomic gases [1, 2, 3] has opened up the study of vortex lattices in a regime which cannot be studied in liquid helium 4. Due to the diluteness of cold atomic gases, it is possible to realize situations in which the vortex core size is comparable to the vortex spacing [4].

In a seminal work, Ho [5] pointed out that the Hamiltonian for a rotating cloud in a harmonic trap has the same form as that for charged particles in a uniform magnetic field. Based on the similarity between these two systems, he argued that when the rotation frequency Ω is close to the transverse frequency $\omega_\perp$ of the trap, almost all particles would condense into the lowest Landau level (LLL) of the Coriolis force. Stimulated by this insight, extensive experimental studies have been performed by the JILA group (see, e.g., Coddington *et al.* [6]), who have achieved angular velocities in excess of $0.99\omega_\perp$ at which the cloud contains a vortex lattice with several hundred vortices [7].

The current frontier of the experiments is entering the mean-field LLL regime in which $\hbar\Omega$ is comparable to or larger than the interaction energy, gn, leading to a system whose wave function is dominated by the LLL component. Here n is the particle density and $g \equiv 4\pi\hbar^2 a_{\rm s}/m$ is the two-body interaction strength, m is the particle mass, and $a_{\rm s}$ is the s-wave scattering length. In this regime, the Gross-Pitaevskii equation is still applicable because the number of particles N is much larger than that of vortices $N_{\rm v}$. As shown by ourselves [8] and confirmed by Cooper *et al.* [9] (see also Ref. [10]), a single-particle wave function of the LLL form is a good approximation to the ground state in the rotating frame, i.e., the yrast state, of rapidly rotating condensates. Even the subtle connection between the vortex lattice distortion and the density profile can be described by the simple LLL approximation: a small distortion of the vortex results in a drastic change of the density profile from Gaussian to the Thomas-Fermi parabola.

However, limitations of the LLL wave function become apparent when we consider excited states. The oscillations of the cloud radius (a so-called breathing mode) in the direction of the rotation axis have been measured in the mean-field LLL regime [7], and those in the transverse direction are expected to be measured in the future experiments. However, the LLL wave function does not have the flexibility to describe these simple collective modes. In the present work, we consider which degrees of freedom in the LLL wave function are relevant to describe the breathing mode and provide a simple improved treatment, which remedies the limitations of the LLL wave function.

In the beginning of the next section, we give the basic formalism of the present analysis: the variational Lagrangian approach [11]. Using this framework, we then discuss the breathing mode of the rapidly rotating two dimensional Bose-Einstein condensates. In Section III, large-amplitude oscillations are discussed. In Section IV, we provide a simple physical understanding of the result. Summary and conclusion are given in Section V. The mode frequency in three dimensions is calculated in Appendix A.

II. GENERAL FORMALISM

Let us first see why the standard LLL wave function cannot describe the breathing mode. For definiteness, we consider purely two-dimensional motion in the plane perpendicular to the rotation axis. We write the condensate wave function ψ in the form $\psi = \sqrt{N}\phi$, where ϕ is normalized such that $|\phi|^2$ integrated over all space is unity. The LLL wave function can be written as

$$\phi_{\rm LLL}(\mathbf{r}) = A_{\rm LLL} \prod_{i=1}^{N_{\rm v}} (\zeta - \zeta_i)\ e^{-r^2/2d_\perp^2}\ , \qquad (1)$$

where the rotation axis is along the z-axis, $\zeta = x + iy$, ζ_i are the vortex positions measured in the laboratory frame, $N_{\rm v}$ is the number of vortices, $\mathbf{r} = (x, y)$, and $d_\perp = \sqrt{\hbar/m\omega_\perp}$ is the transverse oscillator length.

Employing Eq. (1), we find the angular momentum per particle to be given by

$$L_z \simeq \hbar \int d^2r \left(\frac{r^2}{d_\perp^2} - 1 \right) \langle |\phi_{\rm LLL}|^2 \rangle = \hbar \left(\frac{\langle r^2 \rangle}{d_\perp^2} - 1 \right) \ , \tag{2}$$

where $\langle |\phi_{\rm LLL}|^2 \rangle$ is the density profile smoothed over an area of linear size large compared to the vortex separation but smaller than the radial extent of the cloud. For a uniform density of vortices, the density profile has a Gaussian form,

$$\langle |\phi_{\rm LLL}^{\rm G}|^2 \rangle = \nu(r) = \frac{1}{\pi\sigma^2} e^{-r^2/\sigma^2} \ , \tag{3}$$

where σ is the width parameter given by the vortex density $n_{\rm v}$ as $n_{\rm v} = 1/(\pi d_\perp^2) - 1/(\pi\sigma^2)$ [5]. In this case one finds

$$L_z \simeq \hbar \left(\frac{\sigma^2}{d_\perp^2} - 1 \right) \ . \tag{4}$$

In the real situation, interactions distort the lattice and the density profile becomes a Thomas-Fermi parabola [8, 9, 10],

$$\langle |\phi_{\rm LLL}^{\rm TF}|^2 \rangle = \nu(r) = \nu(0) \left(1 - \frac{r^2}{R_\perp^2} \right) \ , \tag{5}$$

with $\nu(0) = 2/\pi R_\perp^2$, where $R_\perp$ is the cloud radius. In this case the angular momentum is

$$L_z \simeq \hbar \left(\frac{R_\perp^2}{3d_\perp^2} - 1 \right) \ . \tag{6}$$

Here the superscripts "G" and "TF" denote that the density profile is Gaussian and Thomas-Fermi, respectively.

Equations (4) and (6) show that, for the LLL wave function, the cloud width parameter σ or the cloud radius $R_\perp$ is fixed if the angular momentum is constant, i.e., the breathing mode cannot be described by the standard LLL wave function.

A. Extended Lowest Landau Level Wave Function

To describe the breathing mode in the rapidly rotating limit, we introduce an extended lowest Landau level wave function, which keeps the LLL form but allows the oscillator length of the trap (i.e., the trap frequency) to be adjustable:

$$\phi_{\rm ex}(\mathbf{r}) = A_{\rm ex} \prod_{i=1}^{N_{\rm v}} (\zeta - \zeta_i) \ \exp \left[- \left(\frac{1}{\lambda^2} - i\beta \right) \frac{r^2}{2d_\perp^2} \right] \ . \tag{7}$$

The dynamical variable λ describes the variation of the particle density. The wave function (7), like the original LLL wave function (1), has a Gaussian smoothed density profile if the lattice is uniform, but with a modified width parameter given by

$$n_{\rm v} = \frac{1}{\pi\lambda^2 d_\perp^2} - \frac{1}{\pi\sigma^2} \ . \tag{8}$$

The other dynamical variable β generates a radial velocity field v_r which causes a homologous change of the density profile [12] and the corresponding velocity is

$$v_r = \frac{\hbar}{m} \frac{\partial}{\partial r} \left(\frac{\beta r^2}{2d_\perp^2} \right) = \frac{\hbar}{m} \frac{\beta}{d_\perp^2} \ r \ . \tag{9}$$

In the present analysis, we use the variational Lagrangian formalism [11]. The Lagrangian per particle consists of the time-dependent part T and the energy functional E:

$$\mathcal{L}[\phi_{\rm ex}] = T[\phi_{\rm ex}] - E[\phi_{\rm ex}] \ , \tag{10}$$

with

$$E[\phi_{\rm ex}] = K[\phi_{\rm ex}] + V[\phi_{\rm ex}] + E_{\rm int}[\phi_{\rm ex}] \ , \tag{11}$$

where K, V, and $E_{\rm int}$ are the kinetic, potential, and interaction energies. Each term in the Lagrangian functional for the extended LLL wave function can be written as

$$\begin{aligned} T[\phi_{\rm ex}] &= \frac{i\hbar}{2} \int d^2r \left[\phi_{\rm ex}^* \frac{\partial \phi_{\rm ex}}{\partial t} - \phi_{\rm ex} \frac{\partial \phi_{\rm ex}^*}{\partial t} \right] \\ &= \frac{\hbar}{2} \int d^2r \left[\sum_{i=1}^{N_{\rm v}} \frac{2(\mathbf{r} - \mathbf{r}_i) \times \dot{\mathbf{r}}_i}{|\mathbf{r} - \mathbf{r}_i|^2} - \frac{\dot{\beta} r^2}{d_\perp^2} \right] |\phi_{\rm ex}|^2 \ , \qquad (12) \\ K[\phi_{\rm ex}] &= -\frac{\hbar^2}{2m} \int d^2r \ \phi_{\rm ex}^* \nabla_\perp^2 \phi_{\rm ex} = -\frac{2\hbar^2}{m} \int d^2r \ \phi_{\rm ex}^* \partial_{\zeta^*} \partial_\zeta \phi_{\rm ex} \end{aligned}$$

$$= \frac{\hbar\omega_\perp}{2}\int d^2r \left(\frac{1}{\lambda^4}+\beta^2\right)\frac{r^2}{d_\perp^2}|\phi_{\rm ex}|^2 \ , \tag{13}$$

$$V[\phi_{\rm ex}] = \frac{m\omega_\perp^2}{2}\int d^2r \ r^2|\phi_{\rm ex}|^2 \ , \tag{14}$$

and

$$E_{\rm int}[\phi_{\rm ex}] = \frac{g_{\rm 2D}}{2}\int d^2r \ |\phi_{\rm ex}|^4 \ , \tag{15}$$

where $g_{\rm 2D}$ is the effective interaction parameter in two dimensions. If the system is uniform in the z-direction, $g_{\rm 2D} = Ng/Z$, where Z is the axial extent of the cloud, while if the system in the z-direction is in the ground state of a particle in a harmonic potential of frequency ω_z, then $g_{\rm 2D} = Ng/(d_z\sqrt{2\pi})$, where $d_z = \sqrt{\hbar/m\omega_z}$ is the oscillator length in the z-direction [13]. The angular momentum per particle for $\phi_{\rm ex}$ is

$$\begin{aligned} L_z[\phi_{\rm ex}] &= \int d^2r \ \phi_{\rm ex}^* \left[\mathbf{r}\times(-i\hbar\nabla_\perp)\right]_z \phi_{\rm ex} \\ &= \hbar\int d^2r \ \phi_{\rm ex}^*(\zeta\partial_\zeta - \zeta^*\partial_{\zeta^*})\phi_{\rm ex} \\ &= \hbar\int d^2r \left(\frac{r^2}{\lambda^2 d_\perp^2}-1\right)|\phi_{\rm ex}|^2 \ . \end{aligned} \tag{16}$$

Let us now consider the first term of Eq. (12), which we denote by T_1. The velocity of the vortex $\dot{\mathbf{r}}_i$ in the laboratory frame has the azimuthal component $v_{\phi,i} \simeq r_i\Omega$ due to the bulk rotation and the radial component $v_{r,i} \simeq \delta R \ \omega r_i/R$, where R is the scale of the radial extent of the cloud, δR and ω are the amplitude and the frequency of the breathing oscillation. Employing the averaged vortex approximation as we will do in the later discussion, only the azimuthal velocity gives a nonzero contribution because the coarse-grained density profile is axisymmetric:

$$T_1 = \hbar\sum_{i=1}^{N_{\rm v}}\int d^2r \ \frac{(\mathbf{r}-\mathbf{r}_i)\times\hat{\boldsymbol{\phi}}_i v_{\phi,i}}{|\mathbf{r}-\mathbf{r}_i|^2}\nu(r) \ , \tag{17}$$

where $\hat{\boldsymbol{\phi}}_i$ is the unit vector of the azimuthal direction measured from vortex i. We can readily see that the integral of T_1 vanishes when the density is uniform. For the inhomogeneous cloud, the dominant contribution of T_1 comes from vortices at $r_i \sim R$; vortices at $r_i \ll R$ give only small contribution because the cancellation of the cross product between different $\mathbf{r}$ is efficient [14]. The integral of T_1 for each vortex at $r_i \sim R$ yields $\sim \int d^2r \ \Omega\nu(r) = \Omega$ because $|\mathbf{r}-\mathbf{r}_i| \sim R$ and $v_{\phi,i} \sim R\Omega$. The number of vortices in the surface region is proportional to $n_{\rm v}\ell R \sim N_{\rm v}\ell/R$, where $\pi\ell^2$ gives the area per vortex. Thus, for a cloud with a large vortex lattice, T_1 scales as

$$T_1 \propto \hbar\Omega N_{\rm v}\frac{\ell}{R} \ , \tag{18}$$

which becomes negligible compared to the second term of Eq. (12) $T_2 \sim \hbar\omega N_{\rm v}$ if $R \gg \ell$, i.e., $N_{\rm v}^{1/2} \gg 1$ [we will see later that $\omega \sim \Omega(\simeq \omega_\perp)$]. In the later discussion, we assume that the vortex lattice is large enough that the effect of T_1 may be neglected.

B. Gaussian Profile

Let us first consider a cloud with a uniform vortex lattice. Using the averaged vortex approximation, we replace $|\phi_{\rm ex}|^2$ in Eqs. (12) - (15) by the smoothed density profile of a cloud (3) with a uniform vortex lattice. We then obtain

$$T[\phi_{\rm ex}^{\rm G}] \simeq -\frac{\hbar}{2}\frac{\dot\beta\sigma^2}{d_\perp^2} \ , \tag{19}$$

$$K[\phi_{\rm ex}^{\rm G}] \simeq \frac{\hbar\omega_\perp}{2}\left(\frac{1}{\lambda^4}+\beta^2\right)\frac{\sigma^2}{d_\perp^2} \ , \tag{20}$$

$$V[\phi_{\rm ex}^{\rm G}] \simeq \frac{\hbar\omega_\perp}{2}\frac{\sigma^2}{d_\perp^2} \ , \tag{21}$$

$$E_{\rm int}[\phi_{\rm ex}^{\rm G}] \simeq \frac{bg_{\rm 2D}}{4\pi\sigma^2} \ , \tag{22}$$

where $b \equiv \langle|\phi_{\rm ex}|^4\rangle/\langle|\phi_{\rm ex}|^2\rangle^2$ is the Abrikosov parameter, which is comparable to unity.

Similarly, Eq. (16) reads

$$L_z[\phi_{\rm ex}^{\rm G}] \simeq \hbar\left(\frac{\sigma^2}{\lambda^2 d_\perp^2}-1\right) \ . \tag{23}$$

Due to the angular momentum conservation, the dynamical variables σ and λ are not independent by Eq. (23). Writing the constant value of L_z as l_z, λ is expressed as

$$\frac{1}{\lambda^2} = \frac{d_\perp^2}{\sigma^2}\left(\frac{l_z}{\hbar}+1\right) \equiv \frac{d_\perp^2}{\sigma^2}l \ . \tag{24}$$

Using Eq. (24) to eliminate λ from the Lagrangian, we obtain

$$\mathcal{L}[\phi_{\rm ex}^{\rm G}] = -\frac{\hbar}{2}\frac{\dot{\beta}\sigma^2}{d_\perp^2} - \left[\frac{\hbar\omega_\perp}{2}\left\{l^2\frac{d_\perp^2}{\sigma^2} + (\beta^2+1)\frac{\sigma^2}{d_\perp^2}\right\} + \frac{bg_{\rm 2D}}{4\pi\sigma^2}\right] . \tag{25}$$

Thus the Euler-Lagrange equations for the dynamical variables β and σ

$$\frac{d}{dt}\left(\frac{\partial\mathcal{L}[\phi_{\rm ex}^{\rm G}]}{\partial\dot{\beta}}\right) - \frac{\partial\mathcal{L}[\phi_{\rm ex}^{\rm G}]}{\partial\beta} = 0 , \tag{26}$$

$$\frac{d}{dt}\left(\frac{\partial\mathcal{L}[\phi_{\rm ex}^{\rm G}]}{\partial\dot{\sigma}}\right) - \frac{\partial\mathcal{L}[\phi_{\rm ex}^{\rm G}]}{\partial\sigma} = 0 , \tag{27}$$

lead to the following equations,

$$\dot{\sigma} = \omega_\perp\beta\sigma , \tag{28}$$

and

$$\left(\frac{\dot{\beta}}{\omega_\perp} + \beta^2 + 1\right)\frac{\sigma^4}{d_\perp^4} - l^2 - \kappa = 0 , \tag{29}$$

respectively; where $\kappa \equiv mbg_{\rm 2D}/(2\pi\hbar^2)$ is the dimensionless interaction strength. Combining the above two equations, we obtain an equation of motion of the cloud width parameter σ:

$$\frac{1}{\omega_\perp^2 d_\perp^4}\sigma^3\,\ddot{\sigma} + \frac{\sigma^4}{d_\perp^4} - l^2 - \kappa = 0 . \tag{30}$$

According to Eq. (30), the cloud width parameter σ_0 in the equilibrium state is given as

$$\sigma_0^4 = d_\perp^4(l^2+\kappa) . \tag{31}$$

We note that this expression coincides with the width parameter of the minimum energy state obtained by a variational calculation in the rotating frame. Now we suppose σ oscillates around σ_0 as

$$\sigma(t) = \sigma_0 + \delta\sigma(t) , \tag{32}$$

and its deviation $\delta\sigma(t)$ is small. Linearizing Eq. (30) with respect to $\delta\sigma$ yields

$$\delta\ddot{\sigma}(t) + (2\omega_\perp)^2\delta\sigma(t) = 0 . \tag{33}$$

Thus the breathing mode frequency ω in the LLL regime for a Gaussian profile is

$$\omega = 2\omega_\perp . \tag{34}$$

This result agrees with what one obtains from calculations based on hydrodynamics if one takes the limit of a trapping potential that is independent of z [15, 16]. In the case of Ref. [15], the polytropic index must be put equal to the value two appropriate for a dilute Bose gas.

It is notable that the interaction energy scales in the same way as the rotational kinetic energy (the l^2 term) in the Lagrangian (25) and in the equation of motion (30) [17]. Thus the interaction energy enters only in the combination $l^2+\kappa$, so it does not affect the frequency of the breathing oscillation [18]. This is a remarkable feature of the two-dimensional system [17].

In the case of a three-dimensional rotating cloud trapped in a potential $V = m\omega_\perp(x^2+y^2)/2 + m\omega_z z^2/2$, the interaction energy is given as $E_{\rm int} \sim 1/(\sigma^2 R_z)$, where R_z is the radius (width parameter) of the cloud in the z-direction when the density profile of this direction is the Thomas-Fermi parabola (Gaussian). Thus, for a non-zero interaction strength, the two-dimensional monopole oscillation in the xy-plane couples with the one-dimensional monopole oscillation along the z-axis whose frequency is $\sqrt{3}\omega_z$ (in the case where the zero-point energy of the z-direction is negligible compared to the interaction energy) and the resulting mode frequency is modified from $2\omega_\perp$ (see Appendix A).

C. Thomas-Fermi Profile

As in the previous section, we adopt the averaged vortex approximation. For the inverted parabolic density profile of Eq. (5) for a distorted vortex lattice, Eqs. (12) - (15) can be written as

$$T[\phi_{\rm ex}^{\rm TF}] \simeq -\frac{\hbar}{2}\frac{\dot{\beta}R_\perp^2}{3d_\perp^2} , \tag{35}$$

$$K[\phi_{\rm ex}^{\rm TF}] \simeq \frac{\hbar\omega_\perp}{2}\left(\frac{1}{\lambda^4} + \beta^2\right)\frac{R_\perp^2}{3d_\perp^2} , \tag{36}$$

$$V[\phi_{\rm ex}^{\rm TF}] \simeq \frac{\hbar\omega_\perp}{2}\frac{R_\perp^2}{3d_\perp^2} , \tag{37}$$

$$E_{\rm int}[\phi_{\rm ex}^{\rm TF}] \simeq \frac{2bg_{\rm 2D}}{3\pi R_\perp^2} . \tag{38}$$

Using the angular momentum conservation:

$$l_z \equiv L_z[\phi_{\rm ex}^{\rm TF}] \simeq \hbar\left(\frac{R_\perp^2}{3\lambda^2 d_\perp^2} - 1\right) , \tag{39}$$

λ can be expressed as

$$\frac{1}{\lambda^2} = 3\frac{d_\perp^2}{R_\perp^2}\left(\frac{l_z}{\hbar} + 1\right) \equiv 3\frac{d_\perp^2}{R_\perp^2} l . \tag{40}$$

Thus the Lagrangian can be written with only $R_\perp$ and β:

$$\mathcal{L}[\phi_{\rm ex}^{\rm TF}] = -\frac{\hbar}{2}\frac{\dot\beta R_\perp^2}{3d_\perp^2} - \left[\frac{\hbar\omega_\perp}{2}\left\{l^2\frac{3d_\perp^2}{R_\perp^2} + (\beta^2+1)\frac{R_\perp^2}{3d_\perp^2}\right\} + \frac{2bg_{\rm 2D}}{3\pi R_\perp^2}\right] \ . \tag{41}$$

The Euler-Lagrange equation for β leads to

$$\dot R_\perp = \omega_\perp \beta R_\perp \ , \tag{42}$$

and that for $R_\perp$ to

$$\left(\frac{\dot\beta}{\omega_\perp} + \beta^2 + 1\right)\frac{R_\perp^4}{d_\perp^4} - 9\ l^2 - 8\kappa = 0 \ . \tag{43}$$

Combining Eqs. (42) and (43), we obtain

$$\frac{1}{\omega_\perp^2 d_\perp^4} R_\perp^3\ \ddot R_\perp + \frac{R_\perp^4}{d_\perp^4} - 9\ l^2 - 8\kappa = 0 \ . \tag{44}$$

The cloud radius $R_{\perp,0}$ in the equilibrium state is thus given as

$$R_{\perp,0}^4 = d_\perp^4(9l^2 + 8\kappa) \ , \tag{45}$$

which coincides with the cloud radius obtained by minimizing the energy in the rotating frame. Again we notice that the interaction energy scales in the same way as the rotational kinetic energy, and it does not affect the breathing mode frequency [18] (see the Appendix for the three-dimensional case).

A linearized equation of motion for a small oscillation of $R_\perp(t) = R_{\perp,0} + \delta R_\perp(t)$ is

$$\delta\ddot R_\perp(t) + (2\omega_\perp)^2\ \delta R_\perp(t) = 0 \ . \tag{46}$$

According to Eq. (46), the breathing mode frequency ω in the LLL regime for a cloud with a Thomas-Fermi profile is also

$$\omega = 2\omega_\perp \ , \tag{47}$$

which coincides with results in the slow rotation regime [15, 16]. It is also noted that this result is in accord with measurements [4] in the slowly rotating regime.

III. NON-LINEAR OSCILLATIONS

In the present section, we consider large-amplitude oscillations. However, we should mention that the several assumptions in the preceding discussion can break down in the non-linear regime even if the mean-field Gross-Pitaevskii theory is still a good approximation, and thus the validity of the result in the present section is limited. First of all, for the extended LLL wave function to be valid, the density should be always low enough to ensure that the interaction energy is much smaller than the energy gap between the LLL and higher Landau levels, i.e., $gn \ll \hbar\omega_\perp$ or $Na_{\rm s}/Z \ll R^2/d_\perp^2$, where R denotes the cloud width or radius. To keep the two-dimensional character of the system, we require $\hbar\omega_z \gg m\dot R^2$; otherwise, oscillations in the z-direction are excited. One should also note the criterion for the first term T_1 in the time-dependent part of the Lagrangian (12) to be negligible compared to the second term T_2. If the amplitude is large, the cloud can shrink significantly as the angular velocity (and T_1) can become large. Feynman's relation gives the angular velocity of the cloud as $\Omega \simeq \hbar/(m\ell^2) \sim \hbar N_{\rm v}/(mR^2)$; then we have $T_1 \sim \hbar\Omega N_{\rm v}^{1/2} \sim \hbar^2 N_{\rm v}^{3/2}/(mR^2)$. Thus the criterion for $T_1 \ll T_2 \sim \hbar\omega_\perp N_{\rm v}$ leads to $R \gg N_{\rm v}^{1/4} d_\perp$.

The equations of motion (30) and (44) for both the Gaussian and Thomas-Fermi profiles can be written as the following general form:

$$\frac{d^2X}{dt^2} + \frac{d}{dX}\left(\frac{X^2}{2} + \frac{X_0^4}{2X^2}\right) = 0 \ , \tag{48}$$

where X denotes σ or $R_\perp$; X_0 corresponds to σ_0 or $R_{\perp,0}$ given by Eqs. (31) and (45), respectively. Here we measure the length and time in units of $d_\perp$ and $\omega_\perp^{-1}$. Equation (48) has the same form as the Newton's equation of motion for a particle moving in a potential $V(X) \equiv X^2/2 + X_0^4/2X^2$ (see Fig. 1). This potential shows the restoring force caused by the first term when the cloud expands and the strong centrifugal repulsion by the second term when the cloud contracts.

Suppose that, at $t = 0$, the cloud has its equilibrium size $X = X_0$ but with velocity $\dot X(0) = \dot X_0$ to excite a breathing oscillation. Thus the initial kinetic and potential energies are $\dot X_0^2/2$ and $V(X_0) = X_0^2$, respectively. The oscillation enters the non-linear regime when $\dot X_0^2/2 \gtrsim X_0^2$ because the potential is no longer approximated by the harmonic one. We thus introduce the "non-linearity parameter" χ as

$$\chi \equiv \frac{\dot X_0^2}{2X_0^2} \ ; \tag{49}$$

$\chi \ll 1$ in the linear regime and $\chi \gtrsim 1$ in the non-linear regime.

Multiplying Eq. (48) by $\dot X$ and writing as $\dot X\ddot X = (1/2)(d\dot X^2/dt)$ and $\dot X(dV/dX) = dV/dt$, we can integrate this equation analytically and finally obtain

$$\begin{aligned} t - t_0 &= \pm\int \frac{dX}{\sqrt{2\{E - V(X)\}}} \\ &= \mp\frac{1}{2}\arctan\left[\frac{E - X^2}{X\sqrt{2\{E - V(X)\}}}\right] \ , \end{aligned} \tag{50}$$

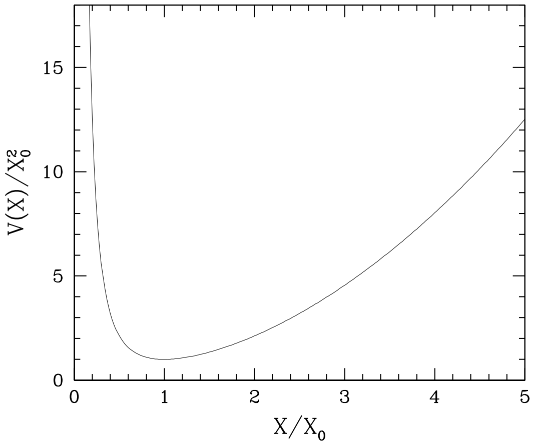

FIG. 1: Effective potential $V(X) = X^2/2 + X_0^4/2X^2$ of the motion of the radial extent of the cloud X.

or

$$\tan\left[\mp 2(t-t_0)\right] = \frac{E - X^2}{X\sqrt{2\{E - V(X)\}}} \, , \tag{51}$$

where t_0 and $E \equiv \dot{X}_0^2/2 + V(X_0) = \dot{X}_0^2/2 + X_0^2$ are the integration constants. We can see from Eq. (51) that the period τ of the oscillation is $\tau = \pi$ (in units of $\omega_\perp^{-1}$) and thus the mode frequency is $2\pi/\tau = 2\pi/(\pi\omega_\perp^{-1}) = 2\omega_\perp$ even in the non-linear regime.

In Fig. 2, we show the time evolution of the width parameter σ and the radius $R_\perp$ of the cloud for some initial conditions. In this plot, we set $l = 100$ and $\kappa = 100$, which are values appropriate for recent experiments [7]. The radial extent of the equilibrium state corresponding to these values of l and κ is $\sigma_0 \simeq 10.02 d_\perp$ for the Gaussian profile and $R_{\perp,0} \simeq 17.36 d_\perp$ for the Thomas-Fermi one. Figure 2(a) shows linear oscillations with $\chi < 1$ and the amplitudes of X are almost symmetric above and below X_0 in the both cases. Figure 2(b) shows a case in the non-linear regime with $\chi = O(10)$. We observe that the oscillations are asymmetric and this feature is more prominent in the Gaussian case than in the Thomas-Fermi one. In Fig. 2(c), we show strongly non-linear oscillations with $\chi > 100$ as a demonstration (however, T_1 is no longer negligible in this case). We can see that the mode frequency $\omega = 2\omega_\perp$ even in the strongly non-linear regime.

IV. PHYSICAL INTERPRETATION OF $\omega = 2\omega_\perp$

In the preceding discussion, we have seen that, in the rapidly rotating regime, the frequency of the breathing mode of a two dimensional cloud is $\omega = 2\omega_\perp$ as in the slow rotation regime [15, 16, 19, 20] (and in the non-rotating case [21]). Furthermore, this result is not limited to small amplitude oscillations. We can understand the above robustness of the result $\omega = 2\omega_\perp$ for the two dimensional rotating cloud in the simplest way by focusing on the orbit of a single particle. Suppose a particle of mass m moves in a circular orbit of radius r. The frequency of oscillations when the circular particle orbit is perturbed can be interpreted as the breathing mode frequency of the cloud. Now we assume that each particle moves in accord with the cloud motion, i.e., $a \equiv r/X$ is constant, where X denotes σ or $R_\perp$ in the case of the Gaussian profile or the Thomas-Fermi one, respectively. In terms of the variable a, the density of the cloud can be written as $n(r) = n(0)\exp(-r^2/\sigma^2) = Na^2\exp(-a^2)/(\pi r^2)$ for the Gaussian profile and $n(r) = n(0)(1 - r^2/R_\perp^2) = 2Na^2(1 - a^2)/(\pi r^2)$ for the Thomas-Fermi one. The interaction energy of a single particle is given by $g_{2\mathrm{D}} n(r) = \gamma/r^2$, where $\gamma \equiv (Ng_{2\mathrm{D}}a^2/\pi)\exp(-a^2)$ in the Gaussian case and $\gamma \equiv (2Ng_{2\mathrm{D}}a^2/\pi)(1 - a^2)$ in the Thomas-Fermi case.

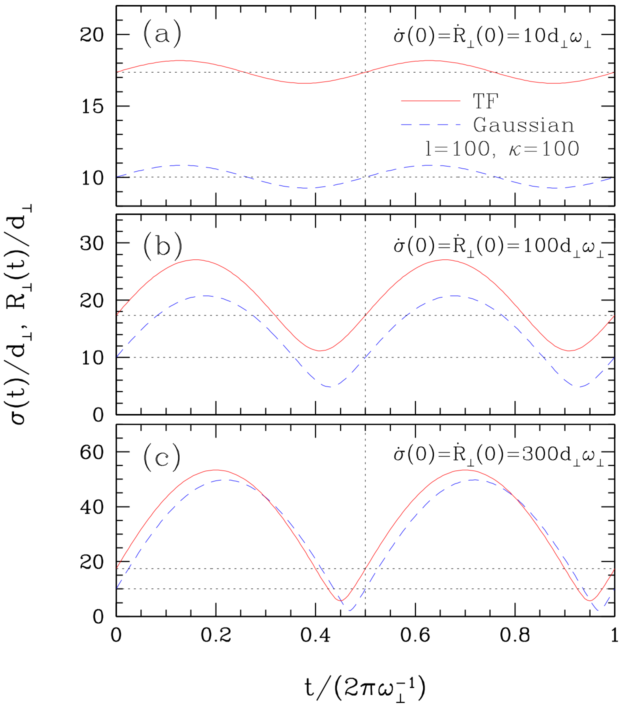

FIG. 2: (Color online) Time evolution of the width parameter σ and the radius $R_\perp$ of the cloud from the linear (a) to the strongly non-linear (c) oscillations.

The energy of the particle is

$$E = \frac{mv^2}{2} + \frac{m\omega_\perp^2}{2}r^2 + \frac{\gamma}{r^2} = \frac{L_z^2}{2mr^2} + \frac{m\omega_\perp^2}{2}r^2 + \frac{\gamma}{r^2} \, , \tag{52}$$

where v is the azimuthal velocity and $L_z = rmv$ is the angular momentum of the particle, which is a constant of motion. The radius r_0 of the unperturbed orbit is given by $\partial E/\partial r|_{r=r_0} = -L_z^2/(mr_0^3) + m\omega_\perp^2 r_0 - 2\gamma/r_0^3 = 0$:

$$r_0^2 = \frac{(L_z^2 + 2m\gamma)^{1/2}}{m\omega_\perp} \, . \tag{53}$$

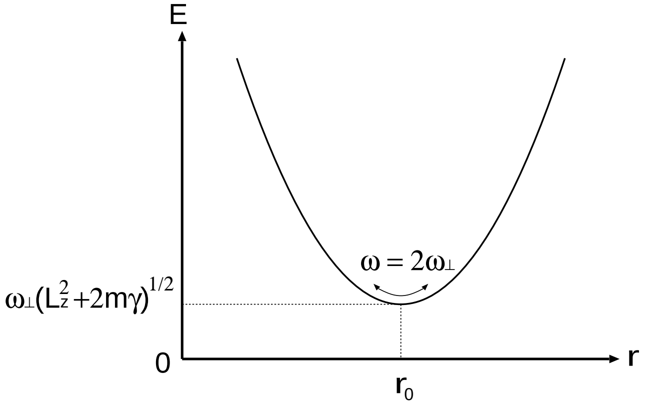

FIG. 3: Schematic picture of the energy of a particle rotating in a harmonic trap of the frequency $\omega_\perp$. Oscillation frequency of the radius of the orbit is $2\omega_\perp$.

We then give a small perturbation δr of r and obtain

$$\begin{aligned} E &\simeq \frac{L_z^2}{2mr_0^2} + \frac{m\omega_\perp^2}{2} r_0^2 + \frac{\gamma}{r_0^2} + \frac{m(2\omega_\perp)^2}{2}\delta r^2 \\ &= \omega_\perp (L_z^2 + 2m\gamma)^{1/2} + \frac{m(2\omega_\perp)^2}{2}\delta r^2 \ , \end{aligned} \tag{54}$$

which is shown schematically in Fig. 3. The first term gives the energy of the unperturbed motion; the second term shows that the frequency of the radial oscillation equals to $2\omega_\perp$. Note that the interaction energy, which has the same r^{-2} dependence as the rotational kinetic energy, just gives a correction to the equilibrium state and it does not affect the dynamics. Thus the breathing mode frequency directly reflects the general property of the rotating single particle motion in two dimensions.

V. SUMMARY AND CONCLUSION

In this work, we have investigated the breathing oscillation of a rapidly rotating two-dimensional Bose-Einstein condensate. Using the variational extended LLL wave function, which incorporates the change of the vortex density, we have shown that the mode frequency is $\omega = 2\omega_\perp$, as in the slow rotation regime. It would be valuable to confirm this prediction in future experiments on rapidly rotating Bose-Einstein condensates. There we have seen that the modulation of the oscillator length in the original LLL wave function is an essential degree of freedom to describe the breathing mode. We have also studied large-amplitude oscillations; we have observed that the amplitude becomes asymmetric due to the nonlinear effect, but the frequency is still $2\omega_\perp$. Finally, we have provided a simple and physical understanding of the result $\omega = 2\omega_\perp$ and its robustness for two-dimensional rotating clouds.

Acknowledgments

The author is grateful to C. J. Pethick for helpful discussion, comments, and support to complete this work. He also thanks V. Schweikhard for a valuable conversation and H. M. Nielsen and L. M. Jensen for helpful discussions. This work was supported in part by the Nishina Memorial Foundation, and by the JSPS Postdoctoral Fellowship for Research Abroad.

APPENDIX A: BREATHING MODE IN THREE DIMENSIONS

We consider the breathing mode in the case of three dimensions and see how the mode frequency is modified from $2\omega_\perp$. In the following analysis, we assume that the radial density profile is the Thomas-Fermi parabola and the axial one is Gaussian. Thus the extended LLL wave function in this case is

$$\begin{aligned} \phi_{\rm ex}(\mathbf{r}) &= A_{\rm ex} \prod_{i=1}^{N_{\rm v}} (\zeta - \zeta_i)\ \exp\left[-\left(\frac{1}{\lambda^2} - i\beta\right)\frac{r^2}{2d_\perp^2}\right] \\ &\quad \times \exp\left[-\frac{z^2}{2\sigma_z^2} + i\gamma\frac{z^2}{2d_z^2}\right] , \end{aligned} \tag{A1}$$

where σ_z is the width parameter of the axial density profile and γ is the dynamical variable describing the velocity field, which causes the homologous change of the axial density profile. The coarse-grained density profile can be written as

$$\langle|\phi_{\rm ex}|^2\rangle = \nu(0)\left(1 - \frac{r^2}{R_\perp^2}\right) e^{-z^2/\sigma_z^2} \ , \tag{A2}$$

with $\nu(0) = 2\pi^{-3/2}/(R_\perp^2\sigma_z)$. The terms in the Lagrangian per particle for the above wave function may be calculated to be

$$\begin{aligned} T[\phi_{\rm ex}] &= \frac{\hbar}{2}\int d^3r \left[\sum_{i=1}^{N_{\rm v}} \frac{2(\mathbf{r}-\mathbf{r}_i)\times\dot{\mathbf{r}}_i}{|\mathbf{r}-\mathbf{r}_i|^2} - \frac{\dot\beta r^2}{d_\perp^2} - \frac{\dot\gamma z^2}{d_z^2}\right] |\phi_{\rm ex}|^2 \\ &\simeq -\frac{\hbar}{2}\left(\frac{\dot\beta R_\perp^2}{3d_\perp^2} + \frac{\dot\gamma\sigma_z^2}{2d_z^2}\right) , \end{aligned} \tag{A3}$$

$$\begin{aligned} K[\phi_{\rm ex}] &= \int d^3r \left[\frac{\hbar\omega_\perp}{2}\left(\frac{1}{\lambda^4}+\beta^2\right)\frac{r^2}{d_\perp^2} + \frac{\hbar\omega_z}{2}\left(\frac{d_z^4}{\sigma_z^4}+\gamma^2\right)\frac{z^2}{d_z^2}\right]|\phi_{\rm ex}|^2 \\ &\simeq \frac{\hbar\omega_\perp}{2}\left(\frac{1}{\lambda^4}+\beta^2\right)\frac{R_\perp^2}{3d_\perp^2} + \frac{\hbar\omega_z}{2}\left(\frac{d_z^4}{\sigma_z^4}+\gamma^2\right)\frac{\sigma_z^2}{2d_z^2}\ , \end{aligned} \tag{A4}$$

$$\begin{aligned} V[\phi_{\rm ex}] &= \frac{m}{2}\int d^3r\ (\omega_\perp^2 r^2 + \omega_z^2 z^2)|\phi_{\rm ex}|^2 \\ &\simeq \frac{\hbar\omega_\perp}{2}\frac{R_\perp^2}{3d_\perp^2} + \frac{\hbar\omega_z}{2}\frac{\sigma_z^2}{2d_z^2}\ , \end{aligned} \tag{A5}$$

and

$$E_{\rm int}[\phi_{\rm ex}] = \frac{g}{2}\int d^3r\ |\phi_{\rm ex}|^4 \simeq \frac{\sqrt{2}}{3\pi^{3/2}}\frac{bg_{\rm 3D}}{R_\perp^2\sigma_z}\ , \tag{A6}$$

with $g_{\rm 3D} = Ng$. The angular momentum per particle is

$$\begin{aligned} L_z[\phi_{\rm ex}] &= \hbar\int d^3r \left(\frac{r^2}{\lambda^2 d_\perp^2} - 1\right)|\phi_{\rm ex}|^2 \\ &\simeq \hbar\left(\frac{R_\perp^2}{3\lambda^2 d_\perp^2} - 1\right)\ , \end{aligned} \tag{A7}$$

which is the same as Eq. (39). Thus the Lagrangian functional can be written as

$$\mathcal{L}[\phi_{\rm ex}] = -\frac{\hbar}{2}\left(\frac{\dot\beta}{3}X^2 + \frac{\dot\gamma}{2}Z^2\right) - \left[\frac{\hbar\omega_\perp}{2}\left\{\frac{3l^2}{X^2} + (\beta^2+1)\frac{X^2}{3}\right\} + \frac{\hbar\omega_z}{2}\left\{\frac{1}{2Z^2} + (\gamma^2+1)\frac{Z^2}{2}\right\} + \frac{4\hbar\omega_\perp}{3}\frac{\kappa_{\rm 3D}}{X^2 Z}\right]\ , \tag{A8}$$

where $X \equiv R_\perp/d_\perp$, $Z \equiv \sigma_z/d_z$, and

$$\kappa_{\rm 3D} \equiv \frac{mbg_{\rm 3D}}{2\pi\hbar^2}\frac{1}{\sqrt{2\pi}d_z} \tag{A9}$$

is the dimensionless interaction strength.

The Euler-Lagrange equations for β and γ lead to

$$\dot X = \omega_\perp \beta X\ , \tag{A10}$$

$$\dot Z = \omega_z \gamma Z\ , \tag{A11}$$

respectively. Using these equations, the equations of motion for X and Z yield

$$\frac{1}{\omega_\perp^2}X^3\ddot X + X^4 - 9l^2 - 8\kappa_{\rm 3D}\frac{1}{Z} = 0\ , \tag{A12}$$

$$\frac{1}{\omega_z^2}Z^2\ddot Z + Z^3 - \frac{1}{Z} - \frac{8\kappa_{\rm 3D}}{3}\frac{\omega_\perp}{\omega_z}\frac{1}{X^2} = 0\ . \tag{A13}$$

The values of X and Z in the equilibrium state, X_0 and Z_0, are given by the following coupled equations $X_0^4 - 9l^2 - 8\kappa_{\rm 3D}Z_0^{-1} = 0$ and $Z_0^3 - Z_0^{-1} - (8\kappa_{\rm 3D}/3)(\omega_\perp/\omega_z)X_0^{-2} = 0$, and linearized equations for small deviations δX and δZ from X_0 and Z_0 are

$$\frac{1}{\omega_\perp^2}X_0^3\delta\ddot X + 4X_0^3\delta X + 8\kappa_{\rm 3D}\frac{\delta Z}{Z_0^2} = 0\ , \tag{A14}$$

and

$$\frac{1}{\omega_z^2}Z_0^2\delta\ddot Z + 3Z_0^2\delta Z + \frac{\delta Z}{Z_0^2} + \frac{16\kappa_{\rm 3D}}{3}\frac{\omega_\perp}{\omega_z}\frac{\delta X}{X_0^3} = 0\ . \tag{A15}$$

Now writing $\delta X = A_X e^{i\omega t}$ and $\delta Z = A_Z e^{i\omega t}$, and using the condition that Eqs. (A14) and (A15) have a nontrivial solution, we finally obtain

$$\begin{aligned} \omega^2 &= \frac{1}{2}\left[\left(3+\frac{1}{Z_0^4}\right)\omega_z^2 + 4\omega_\perp^2\right] \pm \frac{1}{2}\sqrt{\left[\left(3+\frac{1}{Z_0^4}\right)\omega_z^2 + 4\omega_\perp^2\right]^2 - 16\omega_\perp^2\omega_z^2\left(3+\frac{1}{Z_0^4}\right) + \frac{512\kappa_{\rm 3D}^2}{3}\frac{\omega_\perp^3\omega_z}{X_0^6 Z_0^4}} \\ &= \frac{1}{2}\left[\left(3+\frac{1}{Z_0^4}\right)\omega_z^2 + 4\omega_\perp^2\right] \pm \frac{1}{2}\sqrt{\left[\left(3+\frac{1}{Z_0^4}\right)\omega_z^2 + 4\omega_\perp^2\right]^2 - 16\omega_\perp^2\omega_z^2\left(3+\frac{1}{Z_0^4}\right) + 8\omega_\perp^2\omega_z^2\left(1-\frac{9l^2}{X_0^4}\right)}\ . \end{aligned} \tag{A16}$$

We note that the $1/Z_0^4$ terms have come from the zero-point energy in the z-direction. From a variational calculation in the rotating frame, we find $9l^2 = X_0^4\Omega_0^2/\omega_\perp^2$, where Ω_0 is the angular velocity of the cloud in the equilibrium state for a given angular momentum. If one neglects the zero-point energy in the z-direction [22], the above expression reduces to

$$\omega^2 \simeq 2\omega_\perp^2 + \frac{3}{2}\omega_z^2 \pm \frac{1}{2}\sqrt{16\omega_\perp^4 + 9\omega_z^4 - 16\omega_\perp^2\omega_z^2 - 8\omega_z^2\Omega_0^2}\ , \tag{A17}$$

which is exactly the same as Eq. (45) of Ref. [15] (for a polytropic index equal to two) and Eq. (10) of Ref. [16] derived within the hydrodynamic theory in the slow-rotation regime. This agreement justifies our results in the present paper obtained with the extended LLL wave function even for the slow rotation regime. In the breathing mode, only the coarse-grained density and the averaged vortex density are relevant degrees of freedom when the number of vortices is large; the local vortex structure, which cannot be described by the extended LLL in the slow rotation regime, is irrelevant. Unlike the ordinary LLL wave function, the extended LLL wave function can describe the averaged vortex density correctly also in the slow rotation regime due to the extra degree of freedom λ, which is the reason of the above agreement. (In the slow rotation regime, $T_1 \ll T_2$.)

In the rapid rotation limit, where the z-dependence of the wave function corresponds to the ground state of a particle in a harmonic potential, $Z_0 \simeq 1$, and Eq. (A16) leads to

$$\omega^2 \simeq 2\omega_\perp^2 + 2\omega_z^2 \pm 2\sqrt{(\omega_\perp^2 - \omega_z^2)^2 + \frac{1}{2}\omega_z^2(\omega_\perp^2 - \Omega_0^2)}\ . \tag{A18}$$

In the limit of $\Omega_0 \to \omega_\perp$, the two frequencies become $\omega = 2\omega_\perp$ and $\omega = 2\omega_z$. The former value corresponds to the transverse breathing mode and the latter to the axial one. Unlike those for the hydrodynamic models [15, 16], our calculations are therefore able to explain the experimentally obtained change in the axial breathing mode frequency from the value $\omega = \sqrt{3}\omega_z$ given by Eq. (A17) to $2\omega_z$ when the interaction energy per particle falls below $\hbar\omega_z$ [7] (see Ref. [23] for details).

---

[1] M. R. Matthews, B. P. Anderson, P. C. Haljan, D. S. Hall, C. E. Wieman, and E. A. Cornell, Phys. Rev. Lett. **83**, 2498 (1999).

[2] K.W. Madison, F. Chevy, W. Wohlleben, and J. Dalibard, Phys. Rev. Lett. **84**, 806 (2000).

[3] J. R. Abo-Shaeer, C. Raman, J. M. Vogels, and W. Ketterle, Science **292**, 476 (2001).

[4] I. Coddington, P. Engels, V. Schweikhard, and E. A. Cornell, Phys. Rev. Lett. **91**, 100402 (2003).

[5] T.-L. Ho, Phys. Rev. Lett. **87**, 060403 (2001).

[6] I. Coddington, P. C. Haljan, P. Engels, V. Schweikhard, S. Tung, and E. A. Cornell, Phys. Rev. A **70**, 063607 (2004).

[7] V. Schweikhard, I. Coddington, P. Engels, V. P. Mogendorff, and E. A. Cornell, Phys. Rev. Lett. **92**, 040404 (2004).

[8] G. Watanabe, G. Baym, and C. J. Pethick, Phys. Rev. Lett. **93**, 190401 (2004).

[9] N. R. Cooper, S. Komineas, and N. Read, Phys. Rev. A **70**, 033604 (2004).

[10] A. Aftalion, X. Blanc, and J. Dalibard, Phys. Rev. A **71**, 023611 (2005).

[11] V. M. Pérez-García, H. Michinel, J. I. Cirac, M. Lewenstein, and P. Zoller, Phys. Rev. Lett. **77**, 5320 (1996).

[12] Y. Castin and R. Dum, Phys. Rev. Lett. **77**, 5315 (1996).

[13] A. L. Fetter, Phys. Rev. A **68**, 063617 (2003).

[14] Here we consider the physical situation where the vortex lattice extends until $r \sim R$. Even in the case of the Gaussian density profile, vortices do not exist in outer region where the mean-field theory breaks down, i.e., the number of particle per vortex is of order unity or less: $1 \gtrsim \pi\ell^2 n$ ($\pi\ell^2$ is the area per vortex) or $r \gtrsim \sigma[\ln(N\ell^2/\sigma^2)]^{1/2} \sim \sigma[\ln(N/N_{\rm v})]^{1/2}$.

[15] A. Sedrakian and I. Wasserman, Phys. Rev. A **63**, 063605 (2001).

[16] M. Cozzini and S. Stringari, Phys. Rev. A **67**, 041602(R) (2003).

[17] This can be seen also by the following simple argument. In two dimensions, since the angular momentum scales as $L_z = \int d^2r\ \psi^*(\mathbf{r}\times\mathbf{p})\psi \sim \int d^2r\ n(R_{xy}\times mR_{xy}\Omega) \sim m\Omega NR_{xy}^2$, where R_{xy} is the extent of the cloud in the xy-plane, the rotational kinetic energy scales as $K_{\rm rot} \equiv \int d^2r\ \psi^*(m/2)(\mathbf{\Omega}\times\mathbf{r})^2\psi \sim m\Omega^2NR_{xy}^2 \sim L_z^2/(mNR_{xy}^2)$. Similarly, the interaction energy in two dimensions is $E_{\rm int} \equiv (g_{\rm 2D}/2)\int d^2r\ n^2 \sim g_{\rm 2D}N^2/R_{xy}^2$, which has the same $\sim R_{xy}^{-2}$ dependence as $K_{\rm rot}$. Reflecting the fact that rotation is two-dimensional motion, the rotational kinetic energy scales as $K_{\rm rot} \sim L_z^2/(mNR_{xy}^2)$ also in three dimensions because the vector $\mathbf{r}$ in $\mathbf{\Omega}\times\mathbf{r}$ is a transverse vector measured from the rotation axis. However, in three dimensions, the interaction energy scales in a different way from $K_{\rm rot}$ as $E_{\rm int} \equiv (g/2)\int d^3r\ n^2 \sim gN^2/(R_{xy}^2R_z)$, where R_z is the extent of the cloud in the z-direction.

[18] This statement also holds in large-amplitude oscillations as will be seen in Section III. However, in that case, dynamics is determined by the ratio between the radial extent of the cloud in the equilibrium state, which depends on κ and l, and the oscillation amplitude (or the initial velocity of the radial extent of the cloud driving a breathing oscillation). Thus the value of κ reflects in the time evolution of the cloud radius (or the width parameter) in the non-linear oscillation (not so sensitively because the equilibrium width parameter scales as $\sim (l^2+\kappa)^{1/4}$).

[19] S. Choi, L. O. Baksmaty, S. J. Woo, and N. P. Bigelow, Phys. Rev. A **68**, 031605(R) (2003).

[20] T. Mizushima, Y. Kawaguchi, K. Machida, T. Ohmi, T. Isoshima, and M. M. Salomaa, Phys. Rev. Lett. **92**, 060407 (2004).

[21] L. P. Pitaevskii and A. Rosch, Phys. Rev. A **55**, R 853

(1997).
[22] Neglecting the zero-point energy in the z-direction is not consistent with the assumption that the axial density profile is Gaussian. However, as can be seen from the final result, the detail of the density profile does not matter for the frequency of the breathing mode.
[23] G. Watanabe, submitted to Phys. Rev. A (cond-mat/0512317).